



HAL
open science

Electrode effects on the conduction mechanisms in HfO₂-based metal-insulator-metal capacitors

F. El Kamel, P. Gonon, Christophe Vallée, Corentin Jorel

► **To cite this version:**

F. El Kamel, P. Gonon, Christophe Vallée, Corentin Jorel. Electrode effects on the conduction mechanisms in HfO₂-based metal-insulator-metal capacitors. *Journal of Applied Physics*, 2009, 106 (6), pp.064508. 10.1063/1.3226857. hal-00455514

HAL Id: hal-00455514

<https://hal.science/hal-00455514>

Submitted on 16 Mar 2023

HAL is a multi-disciplinary open access archive for the deposit and dissemination of scientific research documents, whether they are published or not. The documents may come from teaching and research institutions in France or abroad, or from public or private research centers.

L'archive ouverte pluridisciplinaire **HAL**, est destinée au dépôt et à la diffusion de documents scientifiques de niveau recherche, publiés ou non, émanant des établissements d'enseignement et de recherche français ou étrangers, des laboratoires publics ou privés.

Electrode effects on the conduction mechanisms in HfO₂-based metal-insulator-metal capacitors

F. El Kamel,^{1,a)} P. Gonon,² C. Vallée,² and C. Jorel²

¹Grenoble Electrical Engineering Laboratory (G2ELab), French National Research Centre (CNRS), 25 Avenue des Martyrs, BP 166, 38042 Grenoble Cedex 9, France

²Microelectronics Technology Laboratory (LTM), CEA/Leti/D2NT/LTM, Joseph Fourier University (UJF), 17 Avenue des Martyrs, 38054 Grenoble Cedex 9, France

(Received 18 August 2009; accepted 19 August 2009; published online 23 September 2009)

The impact of top-electrode metal on the conduction mechanisms of HfO₂ thin films-based metal-insulator-metal capacitors was investigated at temperature ranging from 25 to 150 °C. Al, Cr, and Au are considered as top electrodes whereas Pt constitutes the common bottom electrode. It was found for both capacitors that in the high field region, the leakage mechanism is electrode-limited. The leakage current, measured at the Al/HfO₂ and Cr/HfO₂ interfaces, was largely governed by Fowler–Nordheim tunneling in the whole measured temperature range. The barrier heights, at the Al/HfO₂ and the Cr/HfO₂ interfaces, were around 0.77 and 0.95 eV, respectively. In the case of Au/HfO₂/Pt capacitors, the Au/HfO₂ interface acts as a Schottky barrier with a height of 1.06 eV. © 2009 American Institute of Physics. [doi:10.1063/1.3226857]

I. INTRODUCTION

The ongoing aggressive miniaturization of electronic devices requires reducing the space allowed to these components and consequently increasing the capacitance density per unit area. As the thicknesses of insulators that are commonly used in conventional metal/insulator/metal (MIM) capacitors, such as silicon dioxide and silicon nitride, are being scaled down to their physical limits, a serious problem in modern microelectronics is to replace Si-based dielectrics by the so-called high- κ materials^{1,2} in order to preserve low leakage currents, high breakdown voltage, and good performances. Recently, several promising high- κ candidates, such as Al₂O₃,³ Ta₂O₅,⁴ and HfO₂ (Refs. 5 and 6) to name a few, have been investigated and evaluated by different deposition processes. Among those being studied to date, hafnium dioxide (HfO₂) has emerged as one of the most promising high- κ material for the MIM capacitor applications due to its outstanding characteristics, including excellent thermodynamic stability,⁷ high dielectric constant as compared to SiO₂ and Si₃N₄,⁸ relatively wide band gap⁹ and high breakdown electric field.¹⁰

Although numerous recent works were done on metal/HfO₂/semiconductor metal oxide semiconductor capacitors,^{11–14} there is a lack of information on MIM capacitors,^{9,15} especially in terms of conduction mechanisms. Among the published reports, very little of them studied the effect of top electrode material on the leakage mechanisms and consequently on the device performance. This constitutes the main aim of the present work, where the leakage current measurements were carried out on Al, Cr, Au/HfO₂/Pt MIM capacitors in order to study transport phenomena at the metal/HfO₂ interface.

II. EXPERIMENTAL DETAILS

A set of metal/HfO₂/Pt MIM capacitors were realized. Prcleaned silicon was used as the starting substrate. A bilayer of Ti (10 nm) and Pt (100 nm) was first sputtered at room temperature. Then, HfO₂ films were grown at 350 °C by atomic layer chemical vapor deposition process with alternate cycles of H₂O and HfCl₄ precursors. The deposited films crystallized in the monoclinic phase.⁹ The film thickness (10 nm thick) and the effective optical gap (5.5 eV) were precisely determined using vacuum ultraviolet ellipsometry.⁹ Top electrodes (M =Al, Cr, and Au) were deposited by thermal evaporation through a shadow mask to constitute planar MIM capacitors of 1.77 mm² area. Leakage current measurements were performed on these capacitors as a function of temperature using a Keithley 6517 electrometer. Currents were measured from the top electrode 60 s after the application of dc bias for stabilization concerns. Temperature variation was controlled by a Linkam hot stage. During electrical measurements, the samples were enclosed in a dark shielded cell filled with dry nitrogen gas.

III. RESULTS AND DISCUSSION

Figure 1 shows the results of J - E measurements for different top electrodes at various temperatures with positive bias voltage applied to the Pt bottom electrode. It is important to note that in the high field region, the temperature dependence of the leakage current depends on the electrode nature. For Al and Cr the high-field leakage current weakly depends on T , while for Au the temperature dependence is stronger. In general, basic leakage mechanisms in oxide films can be classified into electrode or bulk limited conduction.¹⁶ In HfO₂-based capacitors, the main current conduction mechanisms are electrode limited, i.e., either Schottky emission,¹¹ Fowler–Nordheim (FN) tunneling¹¹ or also a combination of both. It has also been claimed that the Schottky emission operates at low fields, whereas at high

^{a)}Author to whom correspondence should be addressed. Electronic mail: fadhel.kamel@grenoble.cnrs.fr.

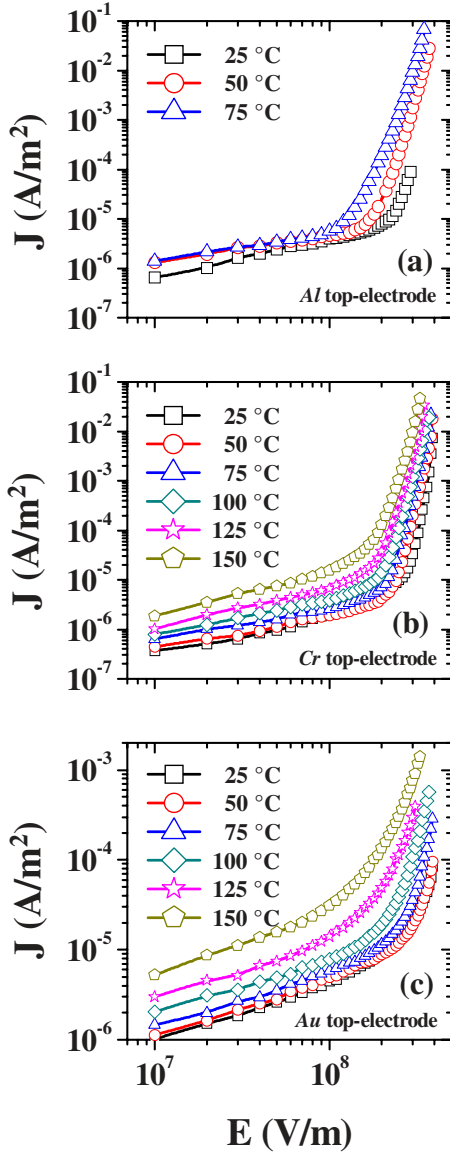


FIG. 1. (Color online) Temperature dependence of the leakage current measured on M/HfO₂/Pt capacitors with different top-electrode metals. (a) M = Al, (b) Cr, and (c) Au. In the high field region the temperature dependence of the leakage current depends on the electrode nature.

fields the FN tunneling dominates the conduction mechanism. In addition, for the high- κ oxides such as HfO₂, the dominant leakage mechanism is usually FN tunneling when the physical thickness is large. As the physical thickness decreases, direct tunneling becomes the more dominant mechanism.¹⁷ After analyzing the experimental data we found that at high electric field the leakage current density, measured on (Al or Cr)/HfO₂/Pt devices, is governed by the FN tunneling and the injection of charge carriers from the top electrode into the HfO₂ layer may take place by tunneling through a triangular energy barrier. The tunneling current can be expressed as¹⁸

$$J = AE^2 \exp\left(\frac{-4\sqrt{2m^*}(q\psi_0)^{3/2}}{3q\hbar E}\right), \quad (1)$$

where J is the current density, E is the applied electric field, A is a constant, q is the elementary charge, $\hbar = h/2\pi$, h is the

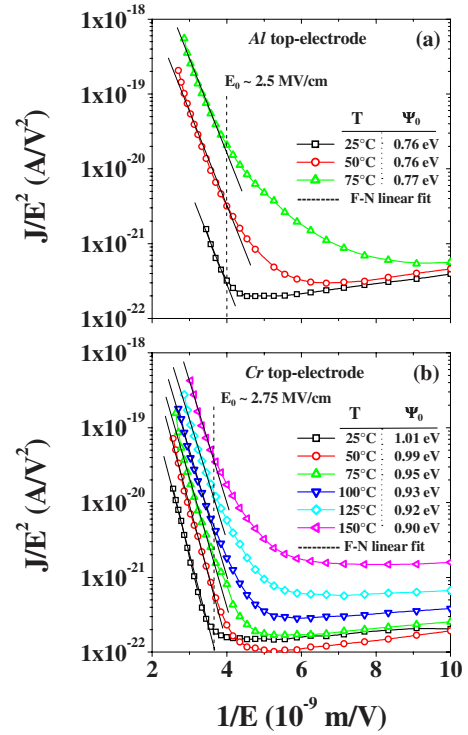


FIG. 2. (Color online) FN tunneling characteristics [$\log(J/E^2)$ vs $1/E$] of (a) Al/HfO₂/Pt and (b) Cr/HfO₂/Pt, replotted from the J - E data. The onset electric field (E_0) of tunneling is quite similar in both capacitors. The interfacial barrier heights, ψ_0 (Al/HfO₂) and ψ_0 (Cr/HfO₂), are listed.

Planck's constant, m^* is the effective electron mass, and ψ_0 is the potential barrier height. If the leakage current is dominated by the FN mechanism, a linear relation between $\ln(J/E^2)$ and $(1/E)$ should therefore be obtained (see Fig. 2). The slope s of the linear fit (FN plot) is a function of the electron effective mass (m^*) and the barrier height (ψ_0), according to the following equation:

$$\psi_0 = \left(\frac{9\hbar^2}{32m^*q}\right)^{1/3} s^{2/3}. \quad (2)$$

In the low voltage region, $\ln(J/E^2)$ curves are nearly flat, while in the high voltage region (above 2.5 MV/cm for Al/HfO₂/Pt and 2.75 MV/cm for Cr/HfO₂/Pt), they increase linearly with $(1/E)$, indicating that the probability of tunneling process becomes larger. The onset electric field (E_0) of tunneling, defined as the threshold at which injection occurs, is quite similar in both capacitors. This implies that carriers injected from the metal electrodes (Al or Cr) toward the conduction band of the HfO₂ films through the potential barrier experience almost the same resistance while top electrodes have different work functions (4.28 eV for Al and 4.5 eV for Cr).

As shown in Eq. (1), the injection current exponentially depends on both the interfacial potential barrier (ψ_0) and the effective mass (m^*) of the tunneling charge carriers in the oxide. Those parameters are crucial when studying the J - E characteristics of the device and therefore accurate values of the effective mass are needed. In the present study we have considered that the electron effective mass in HfO₂ is around $0.4m_0$.^{12,13} So, the interfacial barrier heights, ψ_0 (Al/HfO₂)

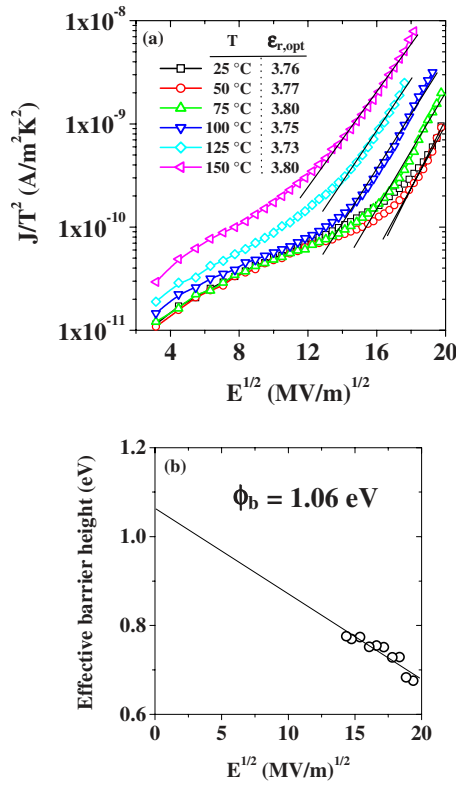


FIG. 3. (Color online) Graph (a) represents the temperature dependence of the Schottky emission plot [$\log(J/T^2)$ vs $E^{1/2}$] based on the experimental J - E data. The dynamic permittivities ($\epsilon_{r,opt}$) calculated from the slope of the fitted straight lines are also listed as a function of the temperature. $\epsilon_{r,opt}$ is close to 3.77 for the entire temperature range. Graph (b) shows the variation in the effective barrier height as a function of the square root of the electric field.

and ψ_0 (Cr/HfO₂), can be extracted using Eq. (2). Data are listed in Figs. 2(a) and 2(b). We note that ψ_0 (Al/HfO₂) is around 0.77 eV and is temperature independent, whereas ψ_0 (Cr/HfO₂) decreases with increasing temperature from 1.01 to 0.90 eV.

Leakage current measurements measured for the Au/HfO₂/Pt capacitors cannot be fitted by a FN law. Instead, in the high field region, the experimental results are fitted by the Schottky emission theory very well, as shown in Fig. 3(a). The leakage current density can be expressed as¹⁹

$$J = AT^2 \exp\left(\frac{-q(\phi_b - \sqrt{qE/4\pi\epsilon_r\epsilon_0})}{k_B T}\right), \quad (3)$$

where J is the current density, $A = 4\pi q m^* k_B^2 / h^3 = 1.2 \times 10^6 (m^*/m_0)(A/m^2 K^2)$, A is the effective Richardson constant, T is the absolute temperature, q is the electronic charge, $q\phi_b$ is the Schottky barrier height, E is the electric field, k_B is the Boltzmann's constant, h is the Planck's constant, ϵ_0 is the permittivity of free space, ϵ_r is the dynamic permittivity (dielectric constant measured in the optic domain), m_0 is the free electron mass, and m^* is the electron effective mass in HfO₂. If the leakage current is governed by the Schottky emission mechanism, a linear behavior between $\ln J$ and $E^{1/2}$ should be obtained, as observe in the high-field domain [see Fig. 3(a)], and the slope will give $\epsilon_{r,opt}$. The dynamic permittivities, calculated at each temperature based on the experimental data, are listed in Fig. 3(a). The ex-

tracted dynamic permittivities and refractive index are respectively close to 3.77 and 1.94 in the temperature range from 25 to 150 °C. These values agree very well with the previous studies.^{12,13} From the Schottky emission model, the barrier height can be determined at a fixed electric field E by plotting $\ln(J/T^2)$ versus $1/T$. The effective barrier height may be given by its slope. In Fig. 3(b) we plotted the effective barrier height as a function of $E^{1/2}$. The linear dependence in the high field region is consistent with the Schottky emission model and an extrapolation of the curve at zero field gives a barrier height of 1.06 eV. Therefore, at high field region the Au/HfO₂ interface acts as a Schottky barrier.

In the high field domain, the distinctive behavior between (Al or Cr)/HfO₂/Pt and Au/HfO₂/Pt leads to conclude that the top metal/HfO₂ interface plays an important role in the conduction process. Recently, the *affinity of metal toward oxygen* has been invoked to explain transport mechanisms at the metal/oxides interfaces.²⁰ It is supposed that metals with high oxygen affinity (as Cr and Al in the present case) are acting as sinks for oxygen, creating more oxygen vacancies. In contrast, Au electrodes have low oxygen affinity and should not react with the HfO₂ layer. Oxygen vacancies, by providing n -type doping, lead to an upward band bending at the electrodes (*a partially depleted layer*). When a dc voltage is applied to the MIM structure, these defects migrate to the cathode creating a positive accumulation layer over a Debye length, $L_D = (\epsilon_0 \epsilon_r k_B T / N q^2)^{1/2}$, where ϵ_r is the relative dielectric constant, N is the density of accumulated charges, and q is their charge. As more and more positive charges accumulate at the cathode, the depletion layer width decreases as $N^{-1/2}$. It is well known that the tunneling probability is dependent on the depletion layer width. The narrower is the layer width, the higher is the tunneling probability. As the barrier is thin enough, it allows tunneling of electrons from the cathode to the dielectric. Thus, when a partially depleted layer forms inside the HfO₂ film (near Al or Cr electrodes), the current is likely to flow through this layer, indicating that the FN tunneling mechanism operates widely in the film. This feature also provides indirect evidence of the formation of a partial depletion layer.

IV. CONCLUSION

In summary, the effect of the top-electrode metal on the conduction mechanisms of HfO₂ thin films-based MIM capacitors was studied at temperature ranging from 25 to 150 °C. The conduction mechanism at the Al/HfO₂ and Cr/HfO₂ interfaces is governed by the FN tunneling with barrier heights of 0.77 and 0.95 eV, respectively. In the case of Au/HfO₂/Pt capacitors, the Au/HfO₂ interface acts as a Schottky barrier with a height of 1.06 eV.

¹G. D. Wilk, R. M. Wallace, and J. M. Anthony, *J. Appl. Phys.* **89**, 5243 (2001).

²J. Robertson, *Eur. Phys. J.: Appl. Phys.* **28**, 265 (2004).

³G. Yip, J. Qiu, W. T. Ng, and Z. H. Lu, *Appl. Phys. Lett.* **92**, 122911 (2008).

⁴H. Shinriki, T. Kisu, S. Kimura, Y. Nishioka, Y. Kawamoto, and K. Mukai, *IEEE Trans. Electron Devices* **37**, 1939 (1990).

⁵S. J. Kim, B. J. Cho, M. F. Li, X. Yu, C. Zhu, A. Chin, and D. L. Kwong, *IEEE Electron Device Lett.* **24**, 6 (2003).

- ⁶H. Hu, C. Zhu, Y. F. Lu, M. F. Li, B. J. Cho, and W. K. Choi, *IEEE Electron Device Lett.* **23**, 345 (2002).
- ⁷K. J. Hubbard and D. G. Schlom, *J. Mater. Res.* **11**, 2757 (1996).
- ⁸H. Iwai, S. Ohomi, S. Akama, C. Ohshima, A. Kikuchi, I. Kashiwagi, J. Tagushi, H. Yamamoto, Y. Kim, I. Ueda, A. Kuriyama, and Y. Yoshihara, *Tech. Dig.- Int. Electron Devices Meet.* **2002**, 625.
- ⁹C. Jorel, C. Vallée, E. Gourvest, B. Pelissier, M. Kahn, M. Bonvalot, and P. Gonon, *J. Vac. Sci. Technol. B* **27**, 378 (2009).
- ¹⁰L. Kang, B. H. Lee, W. J. Qi, Y. Jeon, R. Nieh, S. Gopalan, K. Onishi, and J. C. Lee, *IEEE Electron Device Lett.* **21**, 181 (2000).
- ¹¹H. Wang, Y. Wang, J. Zhang, C. Ye, H. B. Wang, J. Feng, B. Y. Wang, Q. Li, and Y. Jiang, *Appl. Phys. Lett.* **93**, 202904 (2008).
- ¹²H. W. Chen, F. C. Chiu, C. H. Liu, S. Y. Chen, H. S. Huang, P. C. Juan, and H. L. Hwang, *Appl. Surf. Sci.* **254**, 6112 (2008).
- ¹³F. C. Chiu, *J. Appl. Phys.* **100**, 114102 (2006).
- ¹⁴W. J. Zhu, T. P. Ma, T. Tamagawa, J. Kim, and Y. Di, *IEEE Electron Device Lett.* **23**, 97 (2002).
- ¹⁵H. Hu, C. Zhu, Y. F. Lu, Y. H. Wu, T. Liew, M. F. Li, B. J. Cho, W. K. Choi, and N. Yakovlev, *J. Appl. Phys.* **94**, 551 (2003).
- ¹⁶S. M. Sze, *Physics of Semiconductor Devices* (Wiley, New York, 1981).
- ¹⁷M. Houssa, B. De Jaeger, A. Delabie, S. Van Elshocht, V. V. Afanas'ev, J. L. Autran, A. Stesmans, M. Meuris, and M. M. Heyns, *J. Non-Cryst. Solids* **351**, 1902 (2005).
- ¹⁸H. Yang, B. Chen, K. Tao, X. Qiu, B. Xu, and B. Zhao, *Appl. Phys. Lett.* **83**, 1611 (2003).
- ¹⁹H. Yang, K. Tao, B. Chen, X. Qiu, B. Xu, and B. Zhao, *Appl. Phys. Lett.* **81**, 4817 (2002).
- ²⁰H. S. Lee, J. A. Bain, S. Choi, and P. A. Salvador, *Appl. Phys. Lett.* **90**, 202107 (2007).